

Light scattering from an ordered array of needle-shaped organic nanoaggregates: Evidence for optical mode launching

J. Fiutowski,^{a)} V. G. Bordo,^{b)} L. Jozefowski,^{a)} M. Madsen, and H.-G. Rubahn^{c)}

Mads Clausen Institute, NanoSYD, University of Southern Denmark, Alsion 2, DK-6400 Sønderborg, Denmark

(Received 10 November 2007; accepted 11 January 2008; published online 19 February 2008)

Pronounced peaks in both photoluminescence and light scattering from an array of almost parallel oriented, needle-shaped organic nanoaggregates on mica are observed as a function of angle of incidence. Within the framework of a simple theoretical model, we identify those peaks as originating from the launching of normal modes in the nanofibers, both radiative and waveguiding. Quantitative information is obtained about the mode spectrum and morphology of nanoscaled objects from a simple far field scattering measurement. © 2008 American Institute of Physics. [DOI: 10.1063/1.2839396]

In recent years, various classes of light absorbing, light emitting, and/or light guiding nanoaggregates have been reported. Among those are semiconductor quantum dots,¹ carbon nanotubes,² inorganic nanowires,³ and—more recently—organic nanofibers.⁴ Besides their potential use as individual entities with unusual optical or electronic response (e.g., quantum dots) or as arrays with improved optoelectronic performance (e.g., carbon nanotube field emitters⁵), there is also a huge interest in implementing these nanoaggregates into more complex optoelectronic nanocircuits.⁶

In this article, we demonstrate how optical far field technology together with simple theoretical modeling allow one to characterize the nanoaggregates mode spectrum and to validate their ability to represent key waveguiding elements in nanoscaled optoelectronic circuits. As an example, we investigate waveguiding in needleshaped organic nanoaggregates (“nanofibers”). This example is of special interest since organic nanofibers could indeed be important elements for future nanodevices with a large variety of optoelectronic properties. Since the organic fiber growth works with molecules with various functional end groups, fibers with extraordinary high optical gain (leading to random lasing⁷) or pronounced nonlinear optical properties (leading to nanoscaled frequency doublers⁸) can be fabricated.

The excitation of the nanofibers—which eventually leads to their photoluminescence or laser action—can be unambiguously described in terms of the nanofiber normal modes, both radiative and waveguiding.⁹ The intensity of scattered light as well as the electromagnetic energy that penetrates the nanofiber undergo enhancement when the incident radiation is in resonance with such a mode and the phase-matching condition is fulfilled. The mode structure is also reflected in the excitation polarization ratio. A thorough knowledge of the mode dispersion of a given nanofiber ensemble is, therefore, of paramount importance for applications in nanophotonics.

Here, first experimental evidence is given of specific nanofiber mode launching observed in both scattered light

and photoluminescence. To ensure a fixed position of the illuminated spot at the sample when changing the angle of light incidence, we used a half-sphere made of fused silica ($n_s=1.48$ at 325 nm) with a radius of 10 mm. A mica substrate with deposited domains of *para*-hexaphenyl nanofibers was positioned parallel to the planar surface of the half sphere with the help of immersion oil. The nanofibers were deposited on the distant mica side with respect to the half sphere and the sample was oriented such that the nanofiber axes were parallel to the plane of incidence.

We illuminated a flat domain of parallel oriented organic nanofibers with a linearly polarized beam of a He–Cd ($\lambda=325$ nm) laser from the half-sphere side and detected the scattered or emitted light intensity along the normal to the sample surface from the back side (Fig. 1). The extinction ratio of the polarization system is 10^5 . The light beam passed a pinhole of diameter $400\ \mu\text{m}$ and was collimated before entering the half sphere, which results in a beam divergence of less than 0.7° after leaving the half sphere. The angles of incidence were varied between 20° and 65° with respect to the normal axis of the halfsphere.

A photomultiplier mounted on a goniometric table allows us to detect scattered and emitted light intensity distributions from a spot on the sample of a diameter of about $500\ \mu\text{m}$. The acceptance angle of the detection system is 44° . The absolute and relative accuracies of the incident and the detection angles were 1° and 0.5° , respectively. To ob-

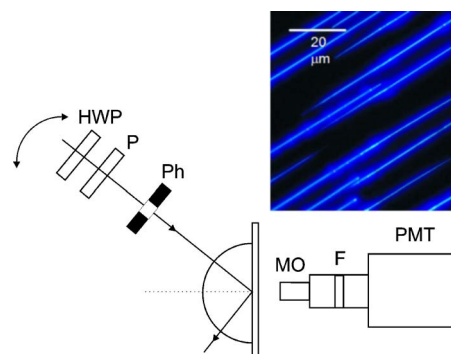


FIG. 1. (Color online) Experimental setup. HWP, half-wave plate; P, polarizer; Ph, pinhole; MO, microscope objective; F, filter; and PMT, photomultiplier. Inset: Fluorescence microscopy image of a sample domain.

^{a)}Permanent address: Marian Smoluchowski Institute of Physics, Jagiellonian University, Reymonta 4, 30-059 Cracow, Poland.

^{b)}Permanent address: A.M. Prokhorov General Physics Institute, Russian Academy of Sciences, 119991 Moscow, Russia.

^{c)}Electronic mail: rubahn@mci.sdu.dk

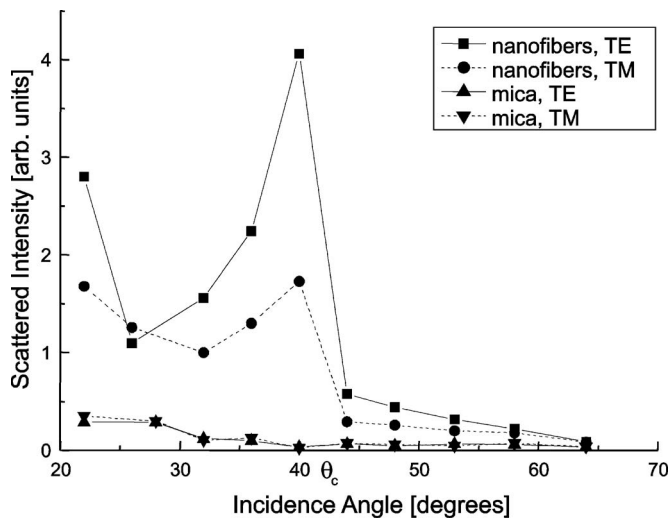


FIG. 2. Intensity of light scattered perpendicularly to the sample surface as a function of the angle of incidence. The incident wave polarization is indicated in the inset.

serve only the wavelengths of interest, we used band pass or interferometric filters in front of the photomultiplier.

The intensity of light *scattered* perpendicularly to the sample surface as a function of the incidence angle θ is shown in Fig. 2. Clear peaks at $\theta=40^\circ$ in both TE and TM incident light polarizations are observed. Those peaks originate from the nanofiber array exclusively as seen from a comparison with the data obtained from a nanofiber-free mica surface. The scattered intensity decreases when the incidence angle exceeds the critical angle for total internal reflection at the quartz hemisphere-air interface, $\theta_c=42.5^\circ$.

The *photoluminescence* intensity measured along the normal to the surface is represented in Fig. 3. Several peaks are seen at both $\theta < \theta_c$ and $\theta > \theta_c$. Some of them (at $\theta=32^\circ$ and at $\theta=58^\circ$) are well pronounced in both polarizations, whereas the others are noticeable in TE polarization only. Figure 4 shows the results of similar measurements but obtained from a different spot on the sample. In this case, the resonance peaks at $\theta=32^\circ$, 44° , and at 58° are distinguishable for TE incident wave polarization only.

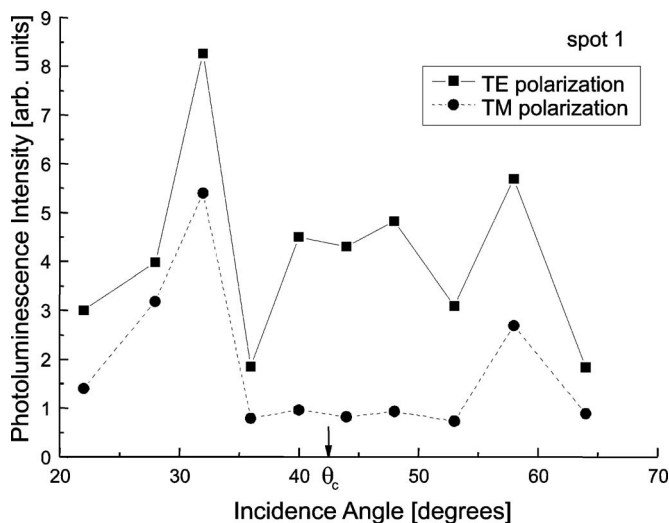


FIG. 3. Photoluminescence intensity measured along the normal to the sample surface as a function of the angle of incidence (spot 1).

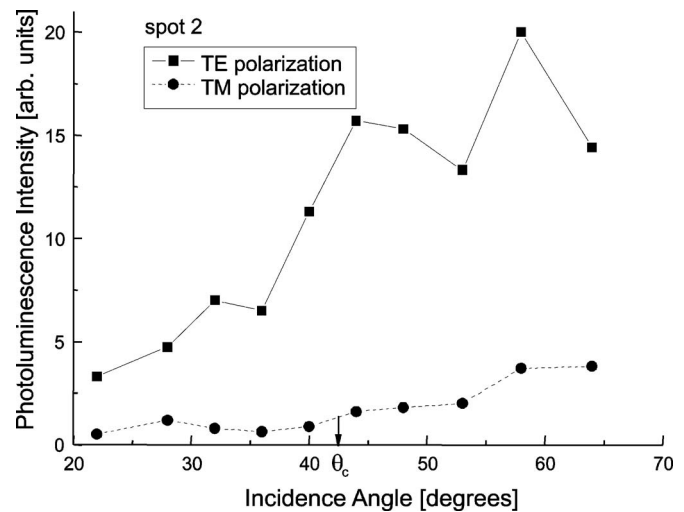


FIG. 4. The same as in Fig. 3, but observed from a different spot on the sample (spot 2).

In order to describe the optical properties of a nanofiber grown on a substrate, we use a model system represented by an infinite isotropic dielectric semicylinder placed on an ideally reflecting surface.¹⁰ Figure 5 shows the dispersion curves of the nanofiber normal modes in dimensionless variables calculated under the assumption that the *para*-hexaphenyl material is isotropic.⁹ They are plotted in the range of size parameters a/λ with a the nanofiber radius and λ the wavelength of the incident radiation corresponding to the experimentally observed typical nanofiber widths ($2a$) as well as the wavelength of the He-Cd laser used for excitation. Here, the dispersion curves of the waveguiding modes lie to the right from the cutoff line $2\pi/\lambda=\beta$ with β the propagation constant. They are denoted as usual in optical waveguide theory.¹¹ The dispersion curves of the radiative modes are located to the left from the cutoff line. For them,

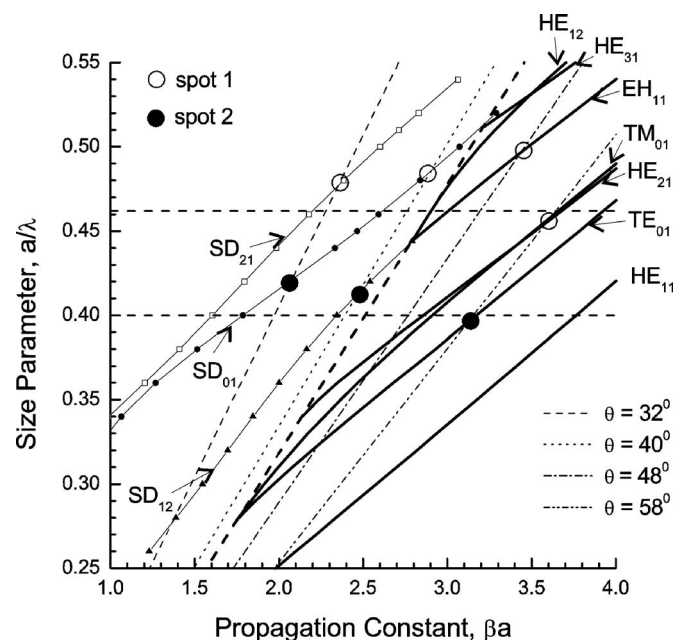


FIG. 5. Dispersion curves of an infinite isotropic dielectric semicylinder placed on an ideally reflecting surface. The bold inclined dashed line indicates the cutoff line. The other inclined straight lines correspond to light incident at the angles shown in the inset. The open and closed circles represent the measured peaks in the photoluminescence experimental data.

the propagation constant is a complex quantity, i.e., $\beta = \beta' + i\beta''$ and only β' is plotted in Fig. 5. The corresponding modes are transient waves decaying along the nanofiber axis; they are called therefore space-decaying modes (SD_{nm}). The condition of the phase matching between the incident light and the nanofiber normal mode can be written as $\beta = (2\pi/\lambda)n_s \sin \theta$. The corresponding dispersion lines for the angles $\theta = 32^\circ, 40^\circ, 48^\circ$, and 58° at which resonances in scattering and photoluminescence are observed are also shown in Fig. 5. Here, all lines corresponding to $\theta < \theta_c$ intersect with the radiation mode curves, whereas those corresponding to $\theta > \theta_c$ cross the waveguide mode curves.

The analysis of the polarization properties of the excited normal modes allows one to specify them. The sharp peak seen in the scattered light intensity at $\theta = 40^\circ$ (Fig. 2) has comparable amplitudes in both TE and TM incident wave polarizations. It can, therefore, be associated with the excitation of the hybrid SD₁₂ mode. The increase in intensity at $\theta < 26^\circ$ originates probably from a resonance with the hybrid SD₂₁ mode. The TE-polarized mode SD₀₁ is suppressed in scattering due to the presence of the reflecting substrate.¹⁰ The comparison of the photoluminescence data shown in Fig. 3 for TE versus TM polarization reveals that the modes excited at $\theta = 32^\circ$ and $\theta = 58^\circ$ are the hybrid modes SD₂₁ and HE₂₁ (probably with admixture of the mode TM₀₁), respectively, whereas the one excited at $\theta = 40^\circ$ is the TE-polarized mode SD₀₁. The line $\theta = 48^\circ$ crosses the dispersion curve EH₁₁ in the relevant domain of the size parameter. However, due to the optical anisotropy of *para*-hexaphenyl nanofibers, the curve HE₁₂ can be shifted closer to the crossing point with the line $\theta = 48^\circ$, which explains the dominance of TE polarization at this resonance. The analysis of the data represented in Fig. 4 reveals that all three resonances at $\theta = 32^\circ, 44^\circ$, and 58° are TE polarized. This observation can be explained if one assumes that the mean size parameter for spot 2 is different from that for spot 1. For spot 2, the intersections with the lines $\theta = 32^\circ$ and $\theta = 58^\circ$ correspond to launching of the modes SD₀₁ and TE₀₁, respectively (see Fig. 5). The broad maximum at $\theta = 44^\circ$ originates very likely from an overlapping of two resonances corresponding to the launching of the modes HE₂₁ and SD₁₂. The positions of the crossing points in Fig. 5 correspond to the most probable size parameter within the illuminated spot shown by the horizontal dashed lines, which results in diameters of about 260 and 300 nm. Both values are within the range of values 240 ± 80 nm obtained from atomic force microscope (AFM) measurements. Due to the approximations of the theoretical model, the crossing points are not situated perfectly on a

straight horizontal line. The broadenings of the isolated peaks observed in photoluminescence allow one to estimate the distribution of the nanofibers in the array over their widths. The angular broadening of about 7° corresponds to a scattering of 0.12λ in nanofiber diameters which gives ~ 40 nm for the relevant wavelength. This value agrees qualitatively with that measured via AFM.

In conclusion, we have demonstrated experimental evidence of mode launching in organic nanofibers grown on mica. Those modes show up as pronounced peaks in both light scattering and photoluminescence from the nanofibers. Using a simple model we are able to identify specific modes which have been excited in the course of light scattering from the sample. Those modes are clearly separated as radiative and waveguiding ones.

The obtained results provide detailed information about possible electromagnetic mode propagation in nanosized, needle-shaped aggregates and form also the basis for a new way of optically characterizing the morphology of subwavelength sized nanostructures via far field scattering. Further development of this technique by using a tunable light source should allow one to determine the actual dispersion curves of nanofibers. Due to its generic nature, the method discussed in this paper is not limited to organic nanofibers but can be equally well applied to other kind of light emitting nanoaggregates.

Financial support of this work from the Danish research councils FTP and FNU is gratefully acknowledged.

- ¹D. V. Regelman, U. Mizrahi, D. Gershoni, E. Ehrenfreund, W. V. Schoenfeld, and P. M. Petroff, *Phys. Rev. Lett.* **87**, 257401 (2001).
- ²J. A. Misewich, R. Martel, Ph. Avouris, J. C. Tsang, S. Heinze, and J. Tersoff, *Science* **300**, 783 (2003).
- ³J. Wang, M. S. Gudiksen, X. Duan, Y. Cui, and C. M. Lieber, *Science* **293**, 1455 (2001); Y. Huang and C. M. Lieber, *Pure Appl. Chem.* **76**, 2051 (2004).
- ⁴F. Balzer and H.-G. Rubahn, *Adv. Funct. Mater.* **15**, 17 (2005).
- ⁵S. Fan, M. G. Chapline, N. R. Franklin, T. W. Tombler, A. M. Cassell, and H. Dai, *Science* **283**, 512 (1999); W. B. Choi, D. S. Chung, J. H. Kang, H. Y. Kim, Y. W. Jin, I. T. Han, Y. H. Lee, J. E. Jung, N. S. Lee, G. S. Park, and J. M. Kim, *Appl. Phys. Lett.* **75**, 3129 (1999).
- ⁶M. Law, D. J. Sirbully, J. C. Johnson, J. Goldberger, R. J. Saykally, and P. Yang, *Science* **305**, 1269 (2004).
- ⁷F. Quochi, F. Cordella, A. Mura, G. Bongiovanni, F. Balzer, and H.-G. Rubahn, *Appl. Phys. Lett.* **88**, 041106 (2006).
- ⁸J. Brewer, M. Schiek, A. Luetzen, K. Al-Shamery, and H.-G. Rubahn, *Nano Lett.* **6**, 2656 (2006).
- ⁹V. G. Bordo, *J. Phys.: Condens. Matter* **19**, 236220 (2007).
- ¹⁰V. G. Bordo, *Phys. Rev. B* **73**, 205117 (2006).
- ¹¹A. W. Snyder and J. D. Love, *Optical Waveguide Theory* (Chapman and Hall, London, 1983).